MEASURING NIGHTTIME ATMOSPHERIC OPACITY USING IMAGES FROM THE MARS EXPLORATION ROVERS

A Senior Scholars Thesis

by

KERI MARIE BEAN

Submitted to the Office of Undergraduate Research
Texas A&M University
in partial fulfillment of the requirements for the designation as

UNDERGRADUATE RESEARCH SCHOLAR

April 2010

Major: Meteorology

MEASURING NIGHTTIME ATMOSPHERIC OPACITY USING IMAGES FROM THE MARS EXPLORATION ROVERS

A Senior Scholars Thesis

by

KERI MARIE BEAN

Submitted to the Office of Undergraduate Research
Texas A&M University
in partial fulfillment of the requirements for the designation as

UNDERGRADUATE RESEARCH SCHOLAR

Approved by:

Research Advisor: Mark Lemmon
Associate Dean for Undergraduate Research: Robert C. Webb

April 2010

Major: Meteorology

ABSTRACT

Measuring Nighttime Atmospheric Opacity Using Images From the Mars Exploration Rovers. (April 2010)

Keri Marie Bean
Department of Atmospheric Sciences
Texas A&M University

Research Advisor: Dr. Mark Lemmon
Department of Atmospheric Sciences

Atmospheric opacity, otherwise known as optical depth, is the measurement of the amount of radiation reaching the surface through the atmosphere. The spatial and temporal patterns in optical depth tell us about the aerosol and cloud cycles in the atmosphere. The water cycle is not well-characterized, so understanding the nature of water vapor and ice in the atmosphere is important. Using images from the Mars Exploration Rover *Spirit*, the nocturnal optical depth was calculated for several bright stars in well-known constellations. The optical depth pattern observed was a 0.2 - 0.8 increase at night and the highest increases were observed around or after local midnight. These observations are consistent with the hypothesis of nocturnal cloud formation. Boundary layer dust and fog are also considered as potential processes for the lower elevation increase.

DEDICATION

This thesis is in dedication to my family, who pushed me towards my dreams.

ACKNOWLEDGMENTS

First off, I would like to acknowledge Dr. Mark Lemmon, my supervising professor, advisor, and mentor, who took me on as a naïve young freshman in 2007 and who, for some reason unbeknownst to me, is helping to guide me to be a successful Martian.

I would also like to thank my parents Thomas and Tracy Bean and my brother Kevin Bean for encouraging me and supporting me towards my goal. I would also like to give a scratch of the ear to my cats Mindy and Misty for tolerating their mom traveling to conferences or staying up late with homework.

If I had to list all the close friends who have helped me, this page would be far too long. I would, however, like to express my thanks to a few friends in particular: Aaron Hope, Rita Matos, and Nicole Sharp have been my best friends and Aggie sports buddies through all these college years, and without them bringing me food late at night while slaving away in the O&M, I would definitely not have survived.

I've had a lot of amazing professors at Texas A&M University, and I'm lucky that I've attended a university where a lot of professors actually care about the students and want them to excel. I'd like to thank Dr. David Sparks and Dr. Michael Tice for letting me help teach UPAS 181 about life on Mars and spending time inspiring some freshman about space exploration. The only 8am class I ever enjoyed, and in fact woke up excited

to attend, was taught by Dr. Shaima Nasiri, and I'd like to thank her for providing an entertaining yet very informative class. Dr. Nasiri's class taught me the basics of physical meteorology, which is the basis of this thesis.

I would also like to thank Texas A&M University and the Department of Atmospheric Sciences for their incredible support over the years. The atmospheric sciences academic advisor Christine Arnold deserves a million thanks for listening to me rant about my research problems and so much more.

NOMENCLATURE

α	Zenith angle
DN	Digital number
I	Observed signal
I_0	Signal at top of atmosphere (absolute magnitude)
L_s	Martian calendar day
λ_{eff}	Maximum efficiency wavelength
M##	Messier catalog object
p	Pressure
Pancam	Panoramic camera
Sol	Day since mission landing
τ	Optical depth
T	Temperature
θ	Angle of object
t	Time

TABLE OF CONTENTS

LIST OF FIGURES

LIST OF TABLES

CHAPTER I

INTRODUCTION

Mars, even with an atmosphere considerably less dense than Earth, has a dynamic weather cycle. Dust storms and clouds have been observed on Mars for decades. The processes behind these weather patterns are still under investigation. Many missions to Mars have studied the atmospheric processes. One of the most common tools for understanding dust concentration and cloud patterns on Mars is by analyzing atmospheric opacity.

Atmospheric opacity, otherwise known as optical depth, is a unitless number that describes how much radiation is scattered and absorbed as it travels through the atmosphere. It is a ratio of the measured intensity of radiation observed to the radiation received at the top of the atmosphere. An optical depth of 0 indicates a perfectly transparent atmosphere; an optical depth of 1 indicates an order of magnitude decrease in detected radiation intensity, and so forth.

Spatial and temporal patterns in optical depth can show clouds, high aerosol concentrations, or other interesting meteorological events. Optical depth is very sensitive to particle concentration and size. Optical depth is also sensitive to particular

---

This thesis follows the style of *Journal of Geophysical Research*.

wavelengths and varies over the electromagnetic spectrum. To determine optical depth, the observed signal from the rover was compared to the apparent magnitudes of the stars. Optical depth was computed using the equation

$$\log(I/I_0) = -\tau/\sin(\alpha) \quad (1)$$

where τ is the optical depth, I is the observed signal by the rovers, I_0 is the signal at the top of the atmosphere, and α is the elevation angle. Nighttime optical depth measurements are taken at various angles, so the elevation angle affects the optical depth measurement and therefore must be accounted for. Figure 1 below shows an example of an optical depth linear fit plot using some of the data from this analysis.

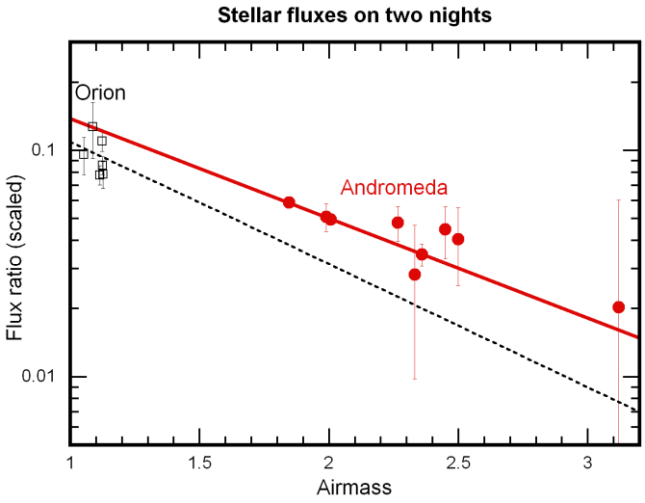

Figure 1 (Linear Fit Optical Depth Plot): A graph depicting the flux ratio on a logarithmic scale compared to the airmass term from equation (1). The red dots indicate the data points for each star in the Andromeda constellation that was analyzed, and the squares represent data points for each star analyzed in the constellation Orion. A linear fit was applied to each data set and the slope of the line represents optical depth.

Optical depth measurements can be used to provide interesting constraints on the dust cycle of Mars. Characterizing the dust cycle is important for understanding energy transport and scattering within the atmosphere [Kahn et al, 1992]. The diurnal dust cycle of Mars is well characterized due to several landed spacecraft. During Spirit's primary mission, an optical depth of 0.9 was observed and this value dropped with a near linear trend through the first 110 sols until the values hovered around 0.5 [Lemmon et al, 2004].

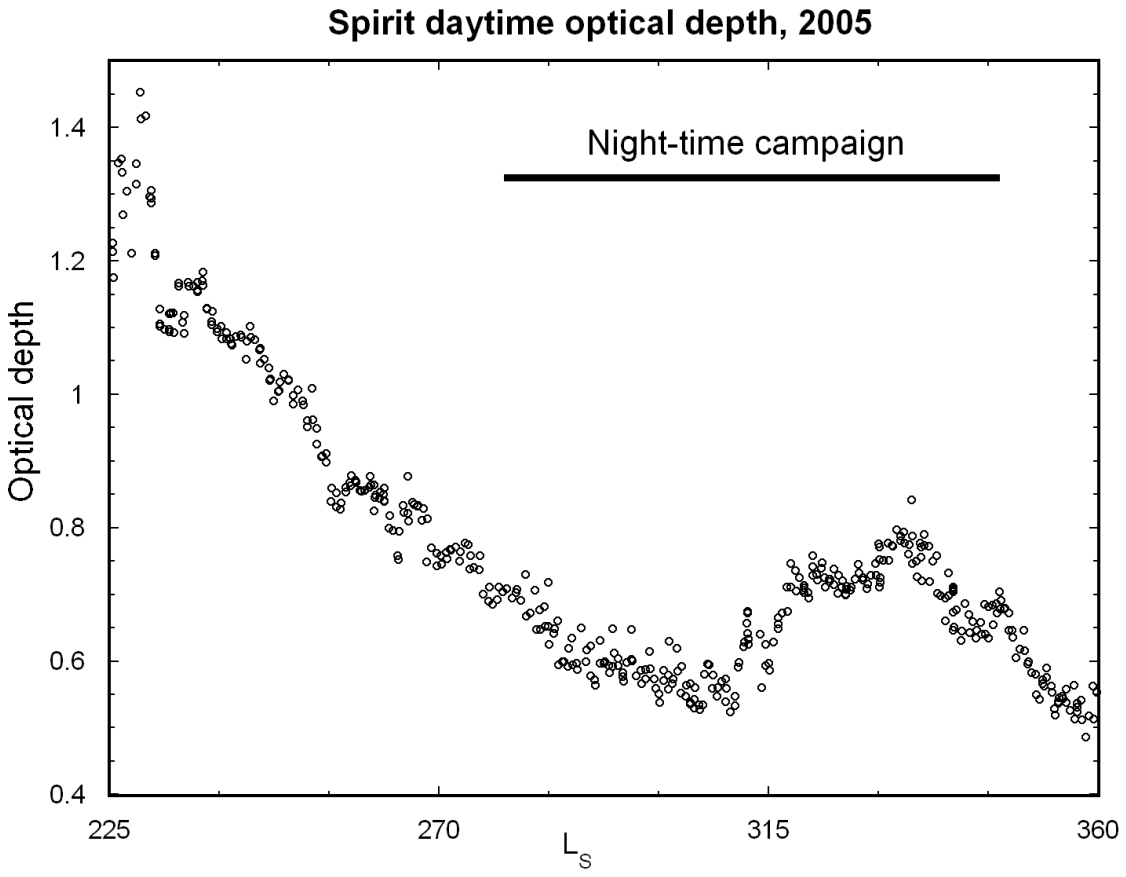

Figure 2 (Daytime Optical Depth Values): Daytime optical depth values from MER-A, Spirit during L_s=225-360. The first major nighttime campaign occurred during the time indicated.

As shown in Figure 2, the average optical depth changes as the seasons change. Figure 2 also shows that during the first nocturnal observation campaigns, daytime optical depths ranged between 0.5 and 0.8. The second campaign had daytime optical values ranging between 0.3 and 0.5. The typical Martian optical depth ranges from 0.1 to 1.0 [Lemmon, 2004].

In addition to the dust cycle, the water cycle is also an important cycle that is actively being researched. The Mars Global Surveyor mission was able to monitor daytime water ice clouds on Mars [Smith, 2004].

The presence of any dust settling or water ice clouds affects optical depth. For example, dust settling decreases optical depth values because less dust would be in the atmosphere to scatter incoming radiation. Clouds increase optical depth values because clouds increase the scattering of radiation and therefore less radiation is detected by the camera. Determining if there are any nocturnal deviations from daytime optical depth would lead to valuable insight in nighttime processes. At night, any of the aforementioned reasons or potentially another unknown process could be in effect.

Nighttime processes are not well constrained due to the difficulty in obtaining consistent nighttime observations. Nighttime optical depth observations must be taken by spacecraft on the ground since the orbiters can only obtain optical depth measurements on the sunlit side of Mars. Only landed spacecraft would be able to take the necessary

images to determine optical depth. Another problem is the power and temperature situation for the landed spacecraft. Taking images at night requires an enormous amount of heating, which implies there must be lots of spare power with a chance to recharge the next sol.

The Mars Pathfinder mission looked at optical depth in both the daytime and nighttime [Smith et al, 1997]. The nighttime observations revealed a slightly higher optical depth than in the daytime which is suspected to be due to water ice crystals forming in the atmosphere [Thomas et al, 1999]. The Phoenix mission used LIDAR observations to verify clouds and precipitation at night in the polar regions [Whiteway et al, 2009].

The Mars Exploration Rovers Spirit and Opportunity have conducted surface operations on Mars for over 5 years now. The daytime characteristics at the locations of Spirit and Opportunity have been well characterized with consistent observations of the Sun [Lemmon et al, 2004]. Due to the longevity of the rovers, nighttime observations have been obtained and can be used to finally gain an understanding of the nocturnal dust cycle in the equatorial regions. Over the course of their mission, they have undertaken imaging campaigns of bright nighttime objects such as Venus, Earth, Mars' two moons Phobos and Deimos, and bright stars such as in Figure 3.

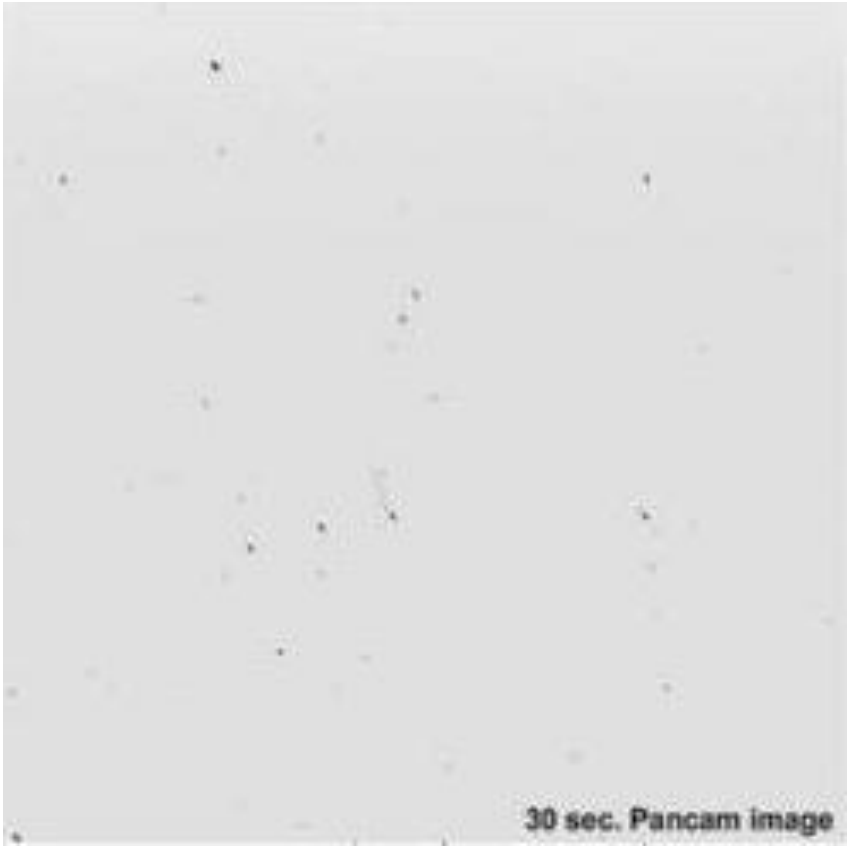

Figure 3 (Orion Constellation (Raw)): A 30 second exposure of the constellation Orion from MER-A, Spirit. This was taken on sol 632 at approximately 12:45am LTST. Image credit: NASA/JPL-Caltech/Cornell/Texas A&M/Space Science Institute

CHAPTER II

IMAGE DATA

The rovers have taken dozens of images of stars, planets, and moons over the course of the mission. Many image sets were of Phobos and Deimos, the Martian moons. Other planets imaged include Earth, Venus, and Jupiter. Spirit imaged several star fields. Specifics on the star fields imaged are seen in Table 1. Opportunity has not made many nighttime observations due to her power situation, so the focus will be on Spirit's observations.

Table 1 (Star Fields Observed by Spirit): The visible stars imaged from Spirit.

Sol number	Stars Observed
632	β Eri, β Ori, δ Ori, κ Ori, ε Ori, ζ Ori, τ Ori, η Ori, ι Ori, ς Ori
661	β Ori
664	α Tau, β Tau
667	α Leo, γ Leo
668	α CMa
694	ε CMa
1941	β And, γ^1 And, μ And
1943, 1949, 1977	α Car

While the images were taken in various filters, the most useful filter was L1. The L1 filter has an effective wavelength of 739nm [Bell et al, 2003]. However, the L1 filter is essentially a blank filter due to the fact it has a large bandpass. The L1 filter detects most visible light and some near infrared light. L1 therefore has the highest sensitivity to point sources since many wavelengths can be detected in a single image. This property is what

makes L1 best suited for star imaging because it allows the most light in, but most challenging for dealing with the broad range of star colors.

Pancam was only designed for daytime imaging of bright scenery. The stars are small, faint point sources. To allow for star detection, longer exposures had to be used. These longer exposures lead to an abnormally high amount of cosmic ray hits, which cause false bright spots in the resulting image and at a quick glance are sometimes indistinguishable from the stars. All of the images needed to be processed carefully to prevent false data. Several exposures of each star field were taken of the course of approximately a half hour period in each observation set. Each observation set was then stacked together. The stars easily stood out in these stacked images because they left distinct star trails in the image, while cosmic rays were random blotches in the images. The stars were marked in the image manually to ensure that cosmic ray hits were not counted as stars. After analyzing the signal to noise ratios, stars below apparent magnitude 4 proved to be too noisy to provide accurate data and are not included in our data set as a result.

CHAPTER III

RESULTS

The consistent result among all the nighttime images is an increase in optical depth from the daytime value, averaging a 0.2 to 0.8 increase. Two star fields are used as examples below.

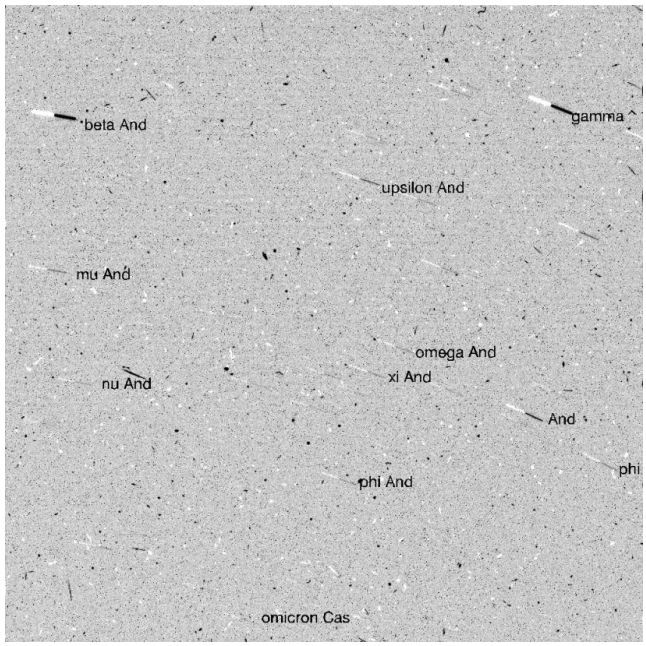

Figure 4 (Andromeda Constellation (Processed)): This compiled image of several exposures of the Andromeda constellation show the distinct star tracks.

Figure 4 shows an image of the Andromeda constellation taken on sol 1941 by Spirit. They were taken from 2:13:00 to 2:26:31 LTST. All of the labeled stars were included in the analysis. For each star track, the optical depth was determined by binning the streak together to obtain a full signal, then computing the optical depth with equation (1). From this observation set, the optical depth was found to be 1.2 ± 0.2. This is approximately a

0.7 increase from the daytime value of 0.498. This observation set was taken at a lower elevation, with an angle of approximately 25°. This observation set is on the higher end of the average increase range.

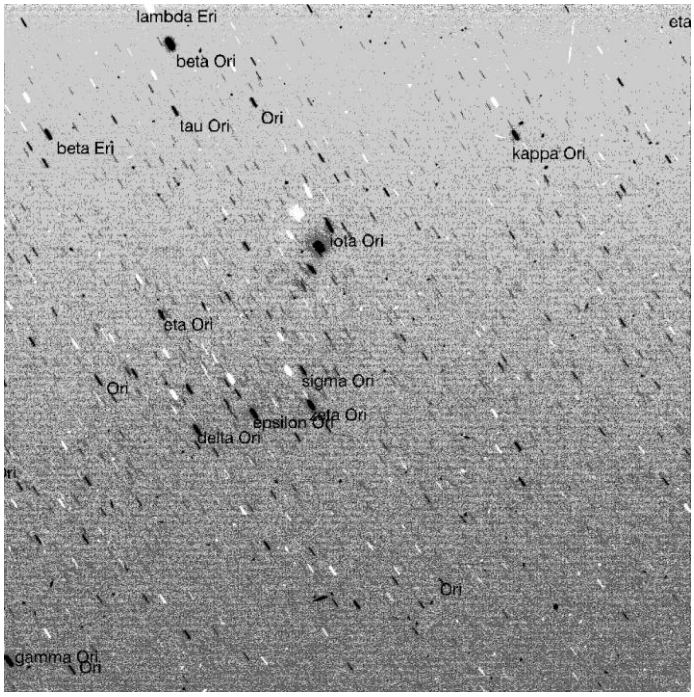

Figure 5 (Orion Constellation (Processed)): This compiled image is of several exposures of the Orion constellation. The star tracks are also visible in this image.

Figure 5 shows the Orion constellation observation set taken from 00:44:30 to 01:02:21 LTST on sol 632. While M42 is a bright object in this image, only the stars were used in determining optical depth to avoid dealing with the nebulosity of M42. The optical depth calculated from this observation set is 1.0 ± 0.1. It has less of an uncertainty due to many more bright stars and was taken at a higher elevation angle of around 60°. This is an approximately 0.4 deviation from the daytime optical depth of 0.581.

Table 2 (Nighttime Optical Depth): This table contains sol number, all of the visible stars observed, the derived optical depth from the respective images, the difference from the observed daytime optical depth, and the local true solar time of the observation.

Sol	Star Name	Optical Depth	Difference in Night vs. Day Optical Depth	Local True Solar Time
632	β Ori	0.945584197	0.364584197	00:44:13
632	β Eri	0.924492733	0.343492733	00:44:13
632	τ Ori	1.052821156	0.471821156	00:44:13
632	κ Ori	2.992798042	2.411798042	00:44:13
632	η Ori	0.90436214	0.32336214	00:44:13
632	ι Ori	0.453189146	-0.127810854	00:44:13
632	ζ Ori	0.906929341	0.325929341	00:44:13
632	δ Ori	0.935312041	0.354312041	00:44:13
632	ς Ori	0.86049163	0.27949163	00:44:13
632	ε Ori	0.848608883	0.26760883	00:44:13
661	β Ori	2.443027613	1.720027613	04:43:13
661	β Ori	3.009565102	2.286565102	04:43:13
661	β Ori	3.086308061	2.363308061	04:43:13
661	β Ori	3.95447886	3.23147886	04:43:13
664	α Tau	2.601340457	1.880340457	1:20:47
667	α Leo	1.022245402	0.291245402	2:50:31
667	γ Leo	0.64143391	-0.08956609	2:50:31
668	α CMa	1.149174854	0.403174854	2:06:05
694	ε CMa	0.3970485	-0.2899515	22:37:31
1941	β And	1.177419041	0.679419041	2:13:00
1941	γ^1 And	1.180127784	0.682127784	2:13:00
1941	μ And	1.02811406	0.53011406	2:13:00
1943	α Car	1.74740461	1.18840461	23:09:54
1949	α Car	1.199785915	0.750785915	22:06:42
1977	α Car	1.021452891	0.672452891	19:40:05

Table 2 lists all of the starts observed and the difference in optical depth. The vast majority of the data shows an increase in optical depth at night. This is consistent with the hypothesis that clouds are forming at night. Any processes that are causing a decrease in optical depth are masked by this increase.

Even though the majority of the images showed an increase in optical depth, there were three cases of a decrease at night, ranging from a 0.01 to 0.3 overall decrease. There were also several cases of increases much greater than one, with increase amounts clustered around 1.1-1.2, 1.7-1.9, 2.2-2.5, and then one lone observation of a greater than 3 increase. All increases greater than 1 occurred close to or after midnight. The colder conditions later at night are more favorable for cloud formation.

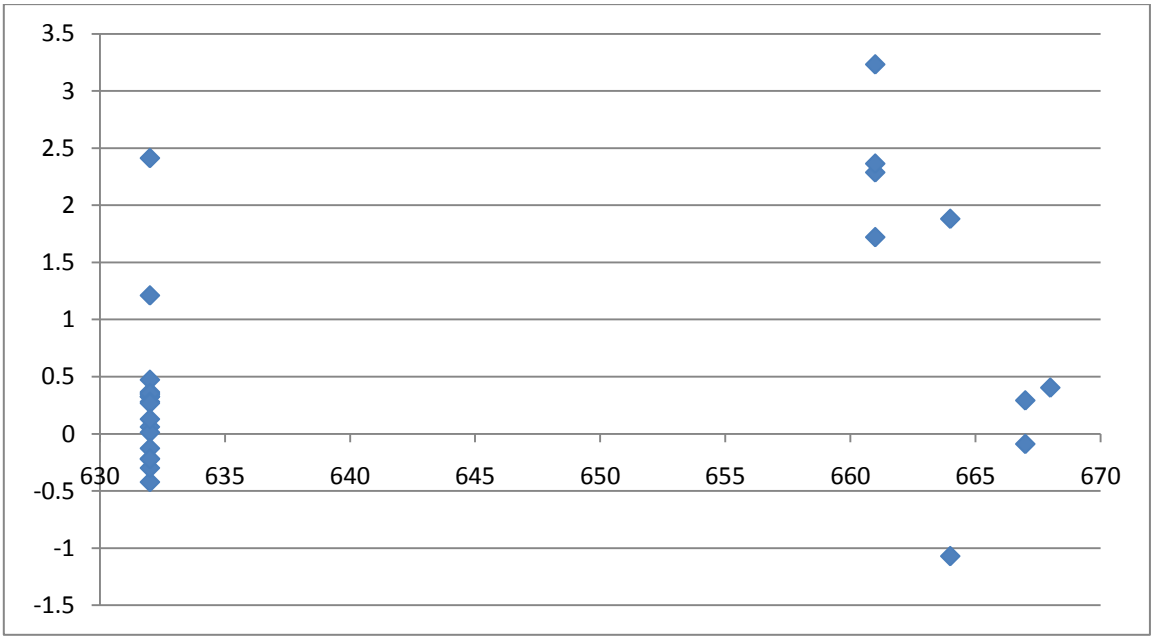

Figure 6 (Optical Depth Difference vs. Sol, First Campaign): This plot shows the scatter in the optical depth difference over the first nighttime optical depth campaign.

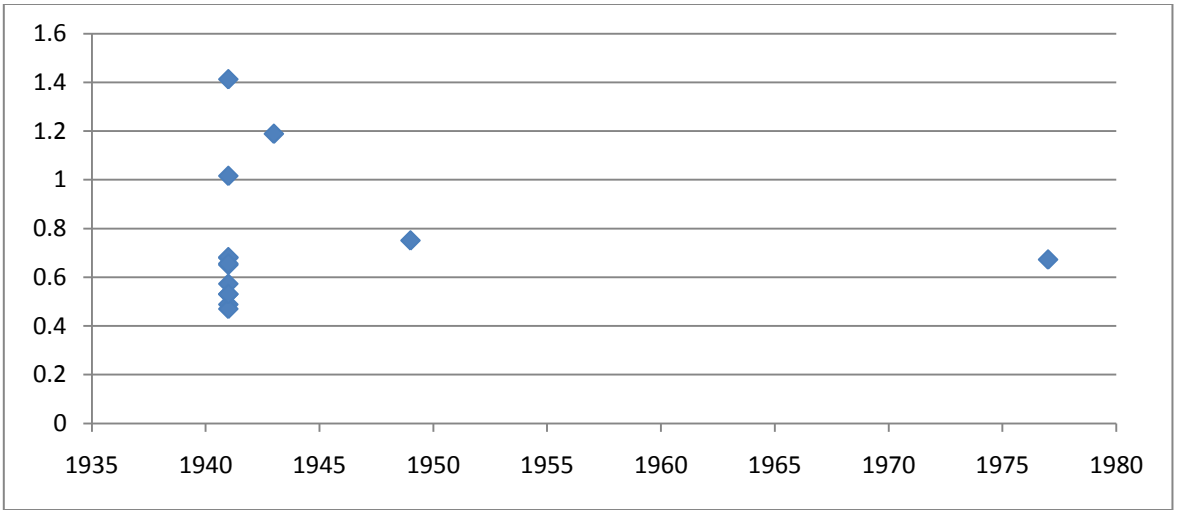

Figure 7 (Optical Depth Difference vs. Sol, Second Campaign): This plot shows the scatter in the optical depth difference over the first nighttime optical depth campaign.

Figures 6 and 7 show the amount of scatter in the optical depth differences. In the first campaign, the optical depth did not vary much from the daytime values, however, in the second campaign, there is a consistent increase, closely ranging between 0.4 and 0.8.

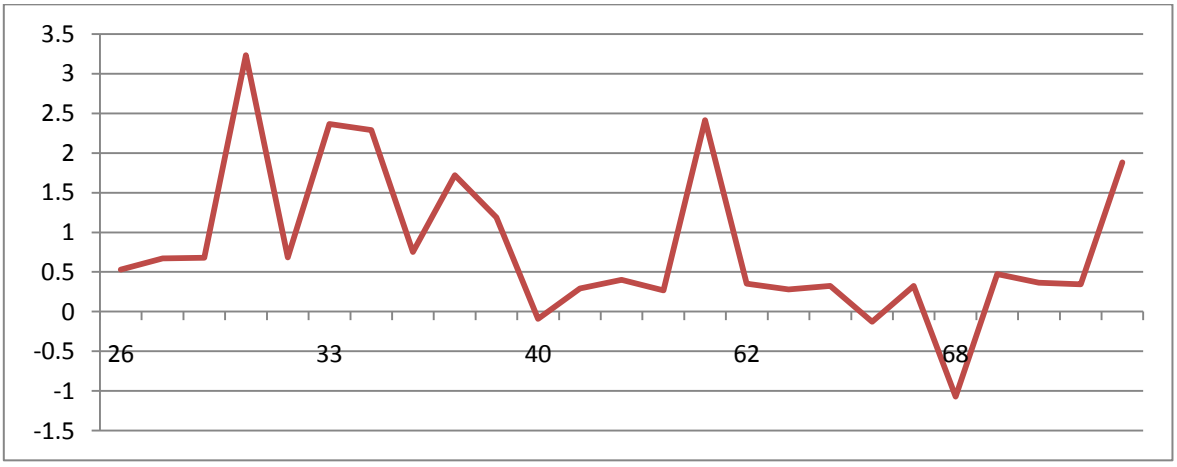

Figure 8: (Optical Depth Difference vs. Elevation Angle): This plot shows the variation in optical depth vs. elevation for all nighttime optical depth images.

Figure 8 shows the optical depth difference as a function of elevation angle. This shows the greater differences concentrating closer to the horizon, and a general trend of smaller increases as elevation angle increases.

CHAPTER IV

SUMMARY AND CONCLUSIONS

The nocturnal atmospheric opacity is now better characterized due to the Mars Exploration Rovers. When comparing the nocturnal optical depths to diurnal optical depths, a 0.2 to 0.8 increase was consistently observed.

All of these observation campaigns were performed in the southern late summer timeframe. The southern late summer is known for being in the later part of dust storm season. It is also long after the normal daytime aphelion cloud belt is observed. If this increase is confirmed by further observations, nocturnal water ice cloud formation is likely the process occurring. This has interesting implications for the water ice cloud cycle. These observation sets do not give any vertical information, therefore the exact thickness and type of cloud layer will require extra observations. It may be impossible to image these nighttime clouds using Pancam due to the high noise in nighttime images.

Figure 8 shows the greatest optical depth differences concentrated closer to the horizon, with the smaller deviations in optical depth as elevation angle increases. The higher elevation images have optical depth increases clustered between 0.2 and 0.6 while lower elevation images have optical depth increases clustered between 0.6 and 0.9. This is consistent with the effect of boundary layer dust. Dust is more concentrated near the surface and trapped within the surface boundary layer. The optical depth path is longer

through this boundary layer, but this path length is corrected by the airmass term from equation (1). To determine if the boundary layer dust is the cause of this increase, follow up observations of taking optical depth measurements at sunrise, before mixing caused by surface heating has a chance to cause a more turbulent boundary layer, would help determine if there is more dust in the boundary layer at night.

Another potential factor for the optical depth increase is the development of localized radiation fog. Fog would also be proportional to airmass, which with the current image sets would show the same increase as boundary layer dust. Fog was observed and further modeled from Viking Lander 1 data [Savijärvi, 1995]. Fog was also observed by the Phoenix Mars Lander, but it required specific meteorological conditions and the polar regions of Mars are considerably colder than Spirit's location [Whiteway et al, 2009]. More commonly, morning radiation fog is caused by orographic features rather than correlating to subsurface water ice or atmospheric water vapor distribution [Möhlmann et al, 2009]. The highest optical depths in the image campaigns were observed between 4am and 5am LTST. While fog can't necessarily be ruled out, the boundary layer dust is a more likely explanation due to the lack of orographic features in Spirit's location that are commonly associated with morning radiation fog. Early morning orbital imaging of the rovers could look for radiation fog to rule this process out.

It is important to note that this increase could be caused by a calibration error. Pancam wasn't originally calibrated for faint point source detection. However, with multiple,

long exposure images, the stars streak across the image. Binning these streaks together help counteract the effect. Also, while L1 is essentially a blank filter, it still has wavelengths that it is more sensitive to. To counteract this effect, color correction would need to be added. The effects of color correction for the observed stars in the L1 filter are still being assessed. Future missions with more sensitive cameras may be able to provide some insight into any calibration issues by taking similar nighttime images of bright stars.

Follow up observations as described above will help confirm the observed optical depth increase and help identify the processes behind the increases. Rechecking calibration and extending the processing and analysis to more nighttime observations not included in this data set will help narrow down and provide more confidence in the potential processes.

REFERENCES

Bell III, J. F., S.W. Squyres, K.E. Herkenhoff, J. N. Maki, H. M. Arneson, et al. (2003), Mars Exploration Rover Athena Panoramic Camera (Pancam) Investigation, *J. Geophys. Res*, *108*(E12), 1703-1709.

Kahn, R. A., T. Z. Martin, R. W. Zurek, S. W. Lee. (1992) The Martian Dust Cycle, *Mars*, 1017-1053.

Lemmon, M. T., M. J. Wolff, M. D. Smith, R. T. Clancy, D. Banfield, *et al*. (2004), Atmospheric Imaging Results from the Mars Exploration Rovers: Spirit and Opportunity, *Science*, *306*(5702), 1753-1756.

Lemmon, M., MER Mars Pancam Atmospheric Opacity RDR V1.0, NASA Planetary Data System, MER1/MER2-M-PANCAM-5-ATMOS-OPACITY-V1.0, 2004.

Möhlmann, D. T. F., M. Niemand, V. Formisano, H. Savijärvi, P. Wolkenberg, (2009), Fog Phenomena on Mars, *Planetary and Space Science*, *57*(14-15), 1987-1992.

Savijärvi, H., (1995), Mars Boundary Layer Modeling: Diurnal Moisture Cycle and Soil Properties at the Viking Lander 1 Site, *Icarus*, *117*, 120-127.

Smith, M. D. (2004), Interannual Variability in TES Atmospheric Observations of Mars During 1999-2003, *Icarus*, *167*(1), 148-165.

Smith, P. H., M. G. Tomasko, D. Britt, D. G. Crowe, R. Reid, et al. (1997), The Imager for Mars Pathfinder Experiment, *J. Geophys. Res.*, *102*(E2), 4003-4025.

Thomas, N., D. Britt, K. Herkenhoff, S. Murchie, B. Semenov, H. Keller, and P. Smith (1999), Observations of Phobos, Deimos, and Bright Stars with the Imager for Mars Pathfinder, *J. Geophys. Res.*, *104*(E4), 9055-9068.

Whiteway, J. A., L. Komguem, C. Dickinson, C. Cook, M. Illnicki, *et al*. (2009), Mars Water-Ice Clouds and Precipitation, *Science*, *325*(5936), 68-70.

CONTACT INFORMATION

Name:	Keri Marie Bean
Professional Address:	c/o Dr. Mark Lemmon Department of Atmospheric Science MS 3150 Texas A&M University College Station, TX 77843
Email Address:	kbean1988@neo.tamu.edu
Education:	B.S., Meteorology, Texas A&M University, May 2010 Undergraduate Research Scholar